Available online at www.sciencedirect.com
SCIENCE DIRECT®
International Journal of Heat and Mass Transfer 49 (2006) 3906–3913
International Journal of HEAT and MASS TRANSFER
www.elsevier.com/locate/ijhmt

Jet impingement cooling of a horizontal surface in a confined porous medium: Mixed convection regime

Nawaf H. Saeid [a,*], Abdulmajeed A. Mohamad [b]

[a] Department of Mechanical Engineering, Curtin University of Technology, CDT 250, 98009 Miri, Sarawak, Malaysia
[b] Department of Mechanical and Manufacturing Engineering, University of Calgary, 2500, Alta., Canada T2N 1N4

Received 28 October 2005; received in revised form 13 March 2006
Available online 30 June 2006

Abstract

In the present article the jet impingement cooling of heated portion of a horizontal surface immersed in a fluid saturated porous media is considered for investigation numerically. The jet direction is considered to be perpendicular from the top to the horizontal heated element; therefore, the external flow and the buoyancy driven flow are in opposite directions. The governing parameters in the present problem are Rayleigh number, Péclet number, jet width and the distance between the jet and the heated portion normalized to the length of the heated element. The results are presented in the mixed convection regime with wide ranges of the governing parameters with the limitation of the Darcy model. It is found for high values of Péclet number that increasing either Rayleigh number or jet width lead to increase the average Nusselt number. Narrowing the distance between the jet and the heated portion could increase the average Nusselt number as well.

No steady-state solution can be found in some cases; when the external jet flow and the flow due to buoyancy are in conflict for domination. The results from the unsteady governing equations in these cases show oscillation of the average Nusselt number along the heated element with the time without reaching steady state.

1. Introduction

The characteristics of the jet impingement cooling through horizontal porous layer are important from theoretical as well as application points of view. In general, convection in porous media has received considerable attention from many researchers due to its wide engineering applications in, for example, insulation of buildings, geothermal engineering, grain storage, solar collectors, electronic components cooling, etc. Representative studies participating to this area and convection heat transfer, in general, can be found in the recent books [1–5].

Free and mixed convection from a horizontal surface in saturated porous media have been a subject of many investigations based on the boundary layer approximations; see for example [6–11]. In these studies, the cooling of the heated horizontal surface is assumed by parallel flow with the heat source. Because Darcy model is valid for low Rayleigh numbers and the boundary layer theory is applicable for high Rayleigh numbers, it is more accurate to consider the full governing equations. Prasad and Kulacki [12], Prasad et al. [13] and Lai et al. [14] have considered the full equations based on Darcy model to study the natural and mixed convection in horizontal porous layer heated from below. They consider the cooling of the heated horizontal surface by parallel flow with the heat source also. Although the literature shows that the jet impingement through pure (non-porous) fluid has been studied extensively (see, for example [15–17]), but it is noticeable that the jet impingement cooling through porous medium has received relatively less attention. Prakash et al. [18] and Fu and Huang [19] have considered the impinging jet studies in enclosures with and without a porous layer. A

* Corresponding author. Present address: School of Mechanical Engineering, University of Nottingham, Malaysia Campus, Samenyih, 43500, Selangor, Malaysia. Tel.: +60 8544 3831; fax: +60 8544 3837.
E-mail address: n_h_saeid@yahoo.com (N.H. Saeid).

0017-9310/$ - see front matter © 2006 Elsevier Ltd. All rights reserved.
doi:10.1016/j.ijheatmasstransfer.2006.03.044

Nomenclature

d	half of the width of the jet, Fig. 1
g	gravitational acceleration
h	distance between the jet and the heated portion, Fig. 1
K	permeability of the porous medium
L	half of the heat source length, Fig. 1
Nu	local Nusselt number, Eq. (9)
$\overline{Nu}$	average Nusselt number along the heat source, Eq. (9)
p	pressure
Pe	Péclet number, $Pe = V_0 L/\alpha$
Ra	Rayleigh number for porous medium, $Ra = g\beta K(T_h - T_c)L/\upsilon\alpha$
s	distances from the heated portion to the end of the solution domain, Fig. 1
t	time
T	temperature
u, v	velocity components along x- and y-axes, respectively
V_0	jet velocity
U, V	non-dimensional velocity components along X- and Y-axes, respectively
x, y	Cartesian coordinates
X, Y	non-dimensional Cartesian coordinates

Greek symbols

α	effective thermal diffusivity
β	coefficient of thermal expansion
θ	non-dimensional temperature
μ	dynamic viscosity
υ	kinematic viscosity
ρ	density
σ	ratio of composite material heat capacity to convective fluid heat capacity
τ	non-dimensional time
ϕ	general dependent variable which can stands for either θ or Ψ
Ψ	non-dimensional stream function

detailed flow visualization experiment has been carried out by Prakash et al. [18] to investigate the effect of a porous layer on flow patterns in an overlying turbulent flow without heat transfer. They studied the effect of the parameters such as the jet Reynolds number, the permeability of the porous foam, the thickness of the porous foam and the height of the overlying fluid layer. Fu and Huang [19] investigated numerically the effects of a laminar jet on the heat transfer performance of three different shape (rectangle, convex and concave) porous blocks mounted on a heated plate. They neglected the buoyancy effects and considered the forced convection mode only. Their results show that the heat transfer is mainly affected by a fluid flowing near the heated region. For a lower porous block, the three types of porous block enhance the heat transfer. However, for a higher porous block, the concave porous block only enhances heat transfer. Recently Jeng and Tzeng [20] studied numerically the air jet impingement cooling of a porous metallic foam heat sink in the forced convection mode. They found the porous aluminum foam heat sink could enhance the heat transfer from the heated horizontal source by impinging cooling. Their results show that the heat transfer performance of the aluminum foam heat sink is 2–3 times larger than that without it. In the present study, the effect of the buoyancy on the jet impingement cooling of heated horizontal surface immersed in a fluid saturated porous media is considered as shown in Fig. 1. The objective of the present study is to characterize the thermal performance of the jet impingement cooling in porous media in the mixed convection regime with the limitation of the Darcy model. The governing parameters in the present problem are the jet width d, the jet velocity V_0, the distance between the jet and the heat source h,

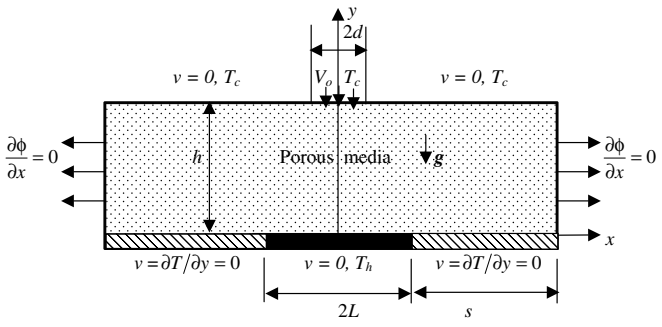

Fig. 1. Schematic diagram of the physical model and coordinate system.

the temperature difference between the heat source and the jet and the heat source length in additional to the physical properties of the porous media and the fluid. These parameters can be reduced to a number of dimensionless groups as given in the next section.

2. Governing equations

To ensure the accuracy of the results, the full two-dimensional equations are considered instead of the boundary layer equations together with the following assumption:

1. The convective fluid and the porous media are in local thermal equilibrium.
2. The properties of the fluid and the porous media are constants.
3. The viscous drag and inertia terms of the momentum equations are negligible, which are valid assumptions for low Darcy and particle Reynolds numbers.

4. The Boussinesq approximation is valid.
5. Darcy law is applicable.

Under these assumptions, the conservation equations for mass, momentum and energy for the two-dimensional steady flow are [1]

$$\frac{\partial u}{\partial x}+\frac{\partial v}{\partial y}=0 \tag{1}$$

$$u=-\frac{K}{\mu}\frac{\partial p}{\partial x} \tag{2a}$$

$$v=-\frac{K}{\mu}\left\{\frac{\partial p}{\partial y}+\rho_0 g[1-\beta(T-T_0)]\right\} \tag{2b}$$

$$u\frac{\partial T}{\partial x}+v\frac{\partial T}{\partial y}=\alpha\left(\frac{\partial^2 T}{\partial x^2}+\frac{\partial^2 T}{\partial y^2}\right) \tag{3}$$

where the subscript 0 for reference point and the Boussinesq approximation $\rho\cong\rho_0[1-\beta(T-T_0)]$ is used in the body force term in Eq. (2b). By eliminating the pressure p from Eqs. (2a) and (2b) a single momentum equation can be derived as

$$\frac{\partial u}{\partial y}-\frac{\partial v}{\partial x}=-\frac{g\beta K}{\upsilon}\frac{\partial T}{\partial x} \tag{4}$$

where υ is the kinematic viscosity μ/ρ_0. Eqs. (1), (3) and (4) may be written in terms of the stream function defined as $u=\partial\psi/\partial y$ and $v=-\partial\psi/\partial x$. Subsequent non-dimensionalisation using

$$U=\frac{u}{V_0}=\frac{\partial\Psi}{\partial Y};\quad V=\frac{v}{V_0}=\frac{-\partial\Psi}{\partial X};\quad \theta=\frac{T-T_c}{T_h-T_c} \tag{5}$$

together with non-dimensionalisation of all the lengths based on the one half of the length of the heated surface (L) and denoting them by respective capital letters leads to the following dimensionless forms of the governing equations:

$$\frac{\partial^2\Psi}{\partial X^2}+\frac{\partial^2\Psi}{\partial Y^2}=\frac{-Ra}{Pe}\frac{\partial\theta}{\partial X} \tag{6}$$

$$\frac{\partial\Psi}{\partial Y}\frac{\partial\theta}{\partial X}-\frac{\partial\Psi}{\partial X}\frac{\partial\theta}{\partial Y}=\frac{1}{Pe}\left(\frac{\partial^2\theta}{\partial X^2}+\frac{\partial^2\theta}{\partial Y^2}\right) \tag{7}$$

where the Rayleigh number and Péclet numbers are defined respectively as $Ra=\frac{g\beta K(T_h-T_c)L}{\upsilon\alpha}$, $Pe=\frac{V_0 L}{\alpha}$.

The flow and heat transfer characteristics are symmetrical around y-axis as shown in Fig. 1. Due to this symmetry, only one half is considered for the computational purpose and the boundary conditions are

$$\partial\Psi(0,Y)/\partial X=\partial\theta(0,Y)/\partial X=0 \tag{8a}$$

$$\partial\Psi(1+S,Y)/\partial X=\partial\theta(1+S,Y)/\partial X=0 \tag{8b}$$

$$\Psi(X,0)=0,\quad \theta(X,0)=1\quad \text{for } 0\leqslant X\leqslant 1$$
$$\text{and otherwise}\quad \partial\theta(X,0)/\partial Y=0 \tag{8c}$$

$$\theta(X,H)=0,\quad \Psi(X,H)=X,\quad \text{for } 0\leqslant X\leqslant D$$
$$\text{and otherwise}\quad \Psi(X,H)=D \tag{8d}$$

The physical quantities of interest in the present investigation are the local and the average Nusselt numbers along the hot surface which are defined respectively as

$$Nu=\left(-\frac{\partial\theta}{\partial Y}\right)_{Y=0};\quad \text{and}\quad \overline{Nu}=\int_0^1 Nu\,dX \tag{9}$$

3. Numerical scheme

Eqs. (6) and (7) subjected to the boundary conditions (8) are integrated numerically using the finite volume method [21]. The central differencing scheme is used for the diffusion terms of the energy equation (7) as well as for the momentum Eq. (6). The quadratic upwind differencing QUICK scheme [22] is used for the convection terms formulation of the energy equation (7). The linear extrapolation, known as mirror node approach, is used for the boundary conditions implementation. The resulting algebraic equations were solved by line-by-line using the Tri-Diagonal Matrix Algorithm iteration. The iteration process is terminated under the following condition:

$$\sum_{i,j}|\phi^n_{i,j}-\phi^{n-1}_{i,j}|\Big/\sum_{i,j}|\phi^n_{i,j}|\leqslant 10^{-5} \tag{10}$$

where ϕ is the general dependent variable which can stands for either θ or Ψ and n denotes the iteration step. The grids are stretched in the X-direction, where steep variations in thermal and velocity fields are expected near the heat source.

To check the accuracy of the present numerical method and the results reported hereafter, energy balance has been employed since no experimental or numerical results were found for this problem. The developed code is essentially a modified version of a code built and validated in previous work [23–25]. The energy balance requires that the heat lost by the lower hot portion must be equal to the heat transferred to the upper cold portion plus the heat being carried out by the fluid at the downstream end. This energy balance can be written in the present formulation as

$$\int_0^1\left(-\frac{\partial\theta}{\partial Y}\right)_{Y=0}dX=\int_0^{1+S}\left(-\frac{\partial\theta}{\partial Y}\right)_{Y=H}dX+Pe\int_0^H\left(\frac{\partial\Psi}{\partial Y}\theta\right)_{1+S}dY \tag{11}$$

The energy balance has been checked for different mesh sizes and the results are presented in Table 1. In Table 1, % error is used to show the percentage error in the energy balance and it means (RHS − LHS) * 100/RHS, where RHS and LHS are the right hand side and the left hand side of Eq. (11) respectively. It is found from Table 1 that the mesh size (151×31) in the X- and Y-directions respectively with $S=4$ gives satisfactory good results. The maximum error in the energy balance is found to be less than 0.4% for the rage of $10\leqslant Pe\leqslant 1000$ and $Ra=100$. The difference in the values of the average Nusselt number

Table 1
Comparison of the results at different mesh sizes with $Ra = 100$, $S = 4$, $D = 0.9$ and $H = 1.0$

Pe	Mesh size (151×31)		Mesh size (301×61)	
	RHS of Eq. (11)	% Error in Eq. (11)	RHS of Eq. (11)	% Error in Eq. (11)
1	3.859	0.196	3.932	0.682
10	1.866	0.235	1.850	0.159
50	5.302	0.375	5.240	0.201
100	7.410	0.008	7.282	0.211
500	16.429	0.040	16.075	0.060
1000	23.207	0.030	22.701	0.040

using (151×31) and (301×61) is around 2%. Moreover, to check if S is large enough to ensure correct exit boundary condition (8b), the computational domain is doubled in X-direction (i.e. $1 + S = 10$) with mesh size (301×61). The results show differences less than 0.05% in the values of average Nusselt number due to duplication of the computational domain and fixed other parameters. Hence $S = 4$ can be considered large enough to get acceptable accurate results and it is fixed with mesh size (151×31) to generate the results hereafter.

4. Results and discussion

The results are presented as average Nusselt number against Péclet number for different values of the parameters Ra, D and H. The range of the parameters are $1 \leqslant Pe \leqslant 1000$, $10 \leqslant Ra \leqslant 100$, $0.1 \leqslant D \leqslant 0.9$ and $0.1 \leqslant H \leqslant 1.0$.

The variation of average Nusselt number with Péclet number for different values of Rayleigh number is shown in Fig. 2 with fixed values of $H = 1$ and $D = 0.1$. In the cases of natural convection domination at low values of Péclet number, the effect of Pe is negligible on the heat transfer process. In this case (natural convection domination), the average Nusselt number can be increased by the increase in the Rayleigh number as shown in Fig. 2 (Note that in Fig. 2, the logarithmic scale is used for both $\overline{Nu}$ and Pe). On contrast to that, at forced convection domination with high values of Pe, Fig. 2 shows that the effect of Rayleigh number is diminished and the variation of $\overline{Nu}$ with Pe for different values of Ra forming a single curve for $Pe > 300$. It can be observed from Fig. 2 that the values of $\overline{Nu}$ and therefore the heat transfer show minimum values for moderate values of Péclet number with high values of Rayleigh number. These values of Pe which result in minimizing the heat transfer are in-between the values of Pe for natural and forced convection domination, which is known as mixed convection. The present mixed convection mode is of opposing nature always since the jet flow is always opposing the buoyant flow. The value of Pe at which minimum $\overline{Nu}$ occurs depends on Ra and at low values of Ra this case where $\overline{Nu}$ shows minimum value is not obvious.

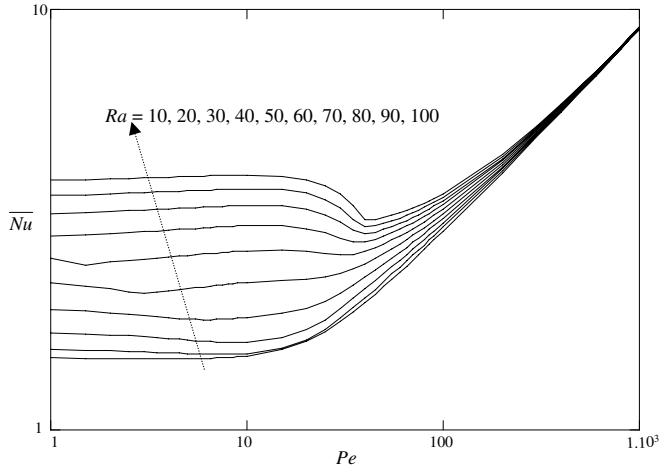

Fig. 2. Variation of average Nusselt number with Péclet number with $H = 1$ and $D = 0.1$.

It is worth mentioning that, in practice, the jet width is usually small comparing with the heated element. Moreover, numerical convergence difficulties encountered for high values of D, especially at high values of Ra where an oscillatory convection is expected as discussed in the next section.

Fig. 3 depicted the details isotherms and streamlines for different values of Pe and fixed values of $H = 1$, $D = 0.1$ and $Ra = 100$, in which the mixed convection mode is clear as presented in Fig. 2. The isotherms and streamlines shown in Fig. 3(a) and (b) for $Pe = 1$ and $Pe = 10$ respectively indicating natural convection domination. The isotherms are cluster near the heat source and two cells rotating the fluid oppositely were formed above the heat source. The streamlines of the jet are comparatively weak and not obvious in theses cases. At $Pe = 40$, Fig. 2 shows that $\overline{Nu} = 3.141$ which is the minimum value for $Ra = 100$, the isotherms and stream lines for this case are shown in Fig. 3(c). At this value of Pe, the flow from the jet modified the flow of the two cells and pushing them away from the heat source. The isotherms are modified as well, where the isotherms above the heat source become approximately parallel to the horizontal, indicating conduction heat transfer mode and hence reducing $\overline{Nu}$. In the forced convection domination, where Pe is high, the two rotating cells disappeared as shown in Fig. 3(d) and (e). The isotherms show high negative gradients; especially in Fig. 3(e), which leads to increase the heat transfer from the heated element.

The effect of the distance from the jet exit to the heat source on the variation of $\overline{Nu}$ with Pe is studied with constant values of other parameters ($D = 0.5$ and $Ra = 50$). For natural convection domination ($Pe < 10$), Fig. 4 shows that $\overline{Nu}$ is approximately constant with the increase in Pe. The effect of the distance H, when $H > 0.7$ is not obvious for $Pe < 10$ and in order to increase the heat transfer the jet (and the upper cold wall) should be closer to the heated element. Fig. 4 shows that values of $\overline{Nu}$ are increasing with the increase of Pe in the forced convection domination mode, similar to that shown in Fig. 2. The variation of

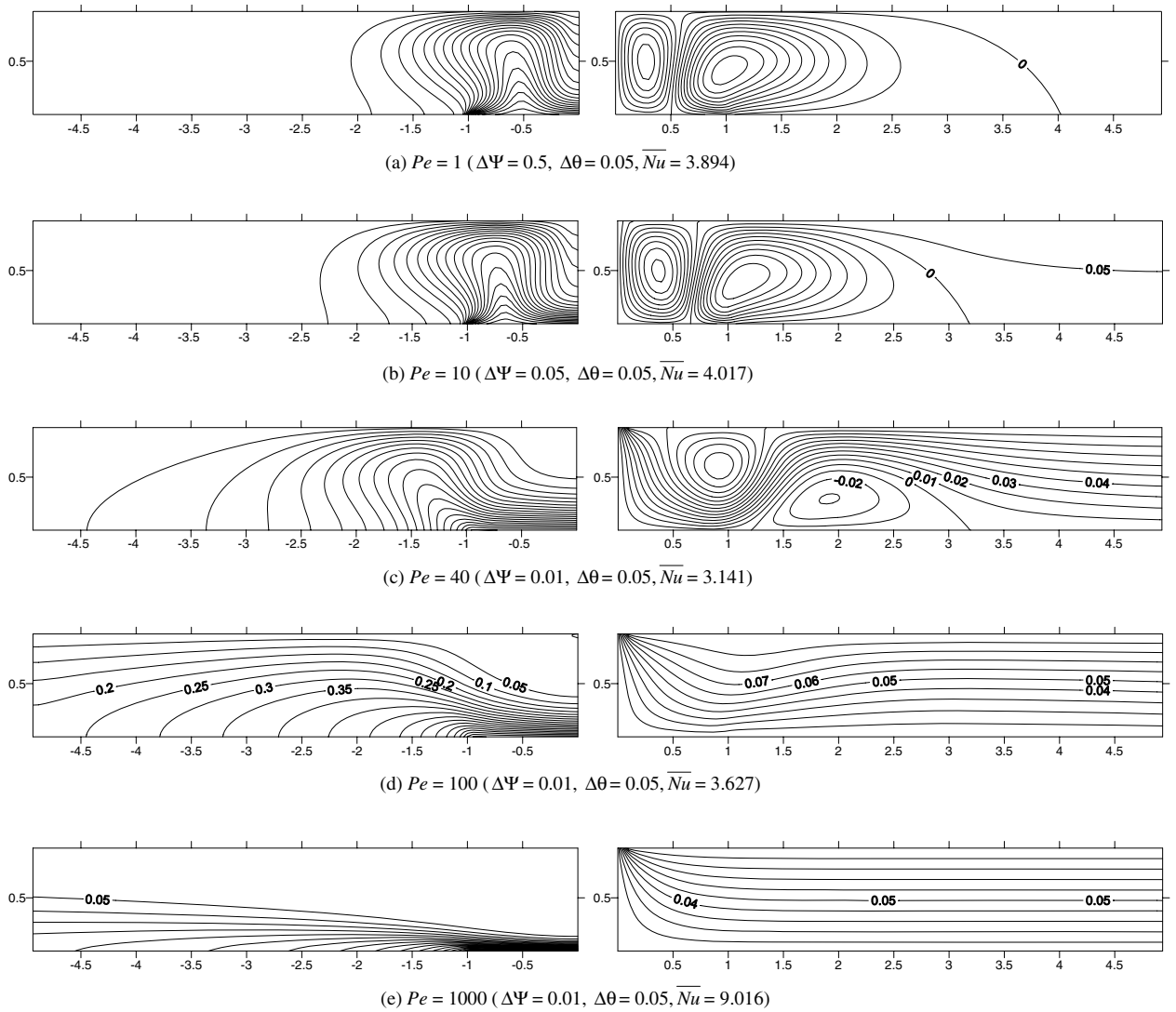

(a) $Pe = 1$ ($\Delta\Psi = 0.5$, $\Delta\theta = 0.05$, $\overline{Nu} = 3.894$)

(b) $Pe = 10$ ($\Delta\Psi = 0.05$, $\Delta\theta = 0.05$, $\overline{Nu} = 4.017$)

(c) $Pe = 40$ ($\Delta\Psi = 0.01$, $\Delta\theta = 0.05$, $\overline{Nu} = 3.141$)

(d) $Pe = 100$ ($\Delta\Psi = 0.01$, $\Delta\theta = 0.05$, $\overline{Nu} = 3.627$)

(e) $Pe = 1000$ ($\Delta\Psi = 0.01$, $\Delta\theta = 0.05$, $\overline{Nu} = 9.016$)

Fig. 3. Isotherms (left), streamlines (right) with $H = 1.0$, $D = 0.1$, and $Ra = 100$.

$\overline{Nu}$ with Pe is linear, when the logarithmic scale is used as shown in Fig. 4. Fig. 4 shows also that narrowing the distance H from 0.2 to 0.1 leads to substantial increase in $\overline{Nu}$. While the enhancement of the heat transfer due to the change of H from 1 to 0.5 is relatively less than that due to narrowing the distance H from 0.2 to 0.1 especially at low values of Pe.

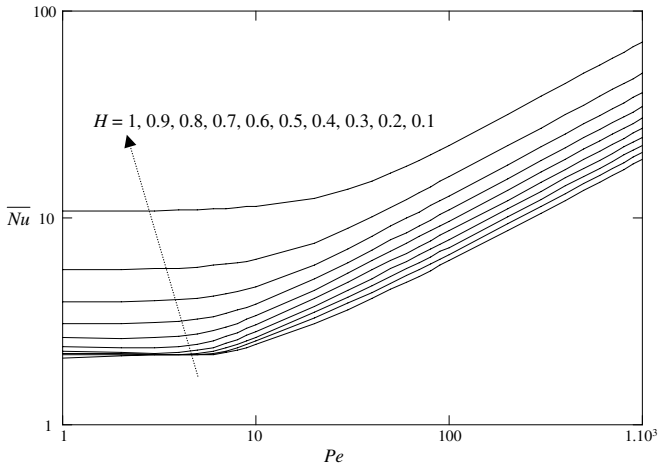

Fig. 4. Variation of average Nusselt number with Péclet number with $D = 0.5$ and $Ra = 50$.

Next, the variation of the average Nusselt number with Péclet number is presented in Fig. 5 with different values of the jet width D and fixed values of $H = 1$ and $Ra = 50$. Fig. 5 shows that at small values of Pe ($Pe < 7$), where the natural convection dominated the average Nusselt number with small jet area is more than that of big jet area. This is due to the fact that small jet area generating weak opposing flow to the buoyant flow for this limits of Pe and Ra. It is observed from Fig. 5 that at $Pe = 7$ same values of $\overline{Nu}$ were found regardless of the values of D. While at $Pe > 7$ (convection domination mode), the average Nusselt number with high values of D is higher than that at small values of D. This indicates the effect of increasing the jet mass flow rate by increasing D and hence increasing the forced convective heat transfer.

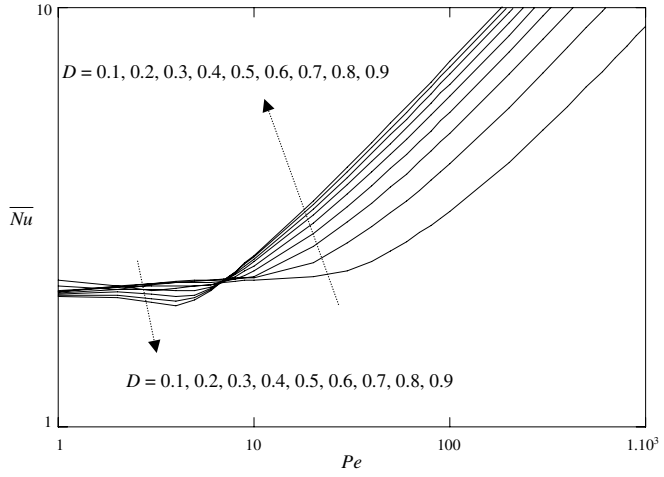

Fig. 5. Variation of average Nusselt number with Péclet number with $H = 1$ and $Ra = 50$.

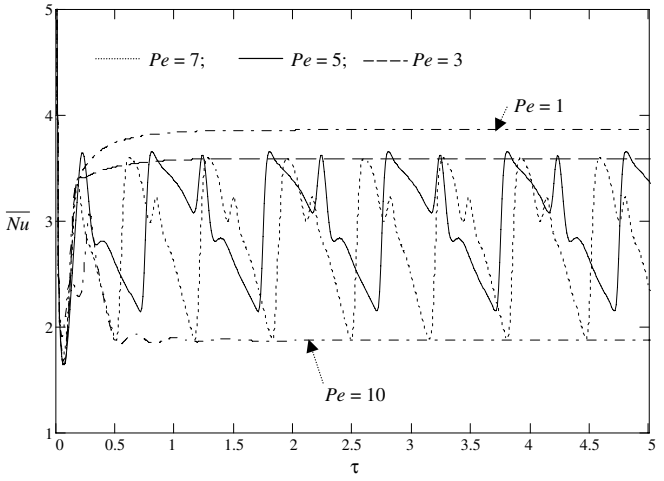

Fig. 6. Transient response of the average Nusselt number with $H = 1$ and $D = 0.9$ and $Ra = 100$.

5. Oscillatory convection

No convergent solution can be obtained for some conditions of the flow when the external jet flow and the flow due to buoyancy are in conflict for domination. This is observed for large jet width, for example $D = 0.9$ with $H = 1$ and high Rayleigh number ($Ra = 100$) with small values of Pe (for example $Pe = 5$). In these cases an oscillatory convection is expected as many mixed convection problems heated from below; see for example [26]. This problem of oscillatory convection needs to be solved using the unsteady set of governing equations. The momentum equation is same as in the steady-state case, Eq. (6) and the energy equation becomes:

$$\frac{\partial\theta}{\partial\tau} + Pe\left(\frac{\partial\Psi}{\partial Y}\frac{\partial\theta}{\partial X} - \frac{\partial\Psi}{\partial X}\frac{\partial\theta}{\partial Y}\right) = \left(\frac{\partial^2\theta}{\partial X^2} + \frac{\partial^2\theta}{\partial Y^2}\right) \tag{12}$$

where $\tau = \alpha t/\sigma L^2$, t is the time and σ is the ratio of composite material heat capacity to convective fluid heat capacity. The initial conditions are assumed to be zero values for both Ψ and θ, the boundary conditions are same as those defined in Eq. (8). The fully implicit scheme is used with time step $\Delta\tau = 0.01$ and the results show negligible differences with $\Delta\tau = 0.001$. Although the same momentum Eq. (6) is used for both steady-state and oscillatory flow, but in the unsteady state the thermal field will affect the velocity field due to the buoyant term in Eq. (6). In the numerical solution the momentum and energy equations are solved simultaneously at each time step and, therefore, the velocity field instantly response to the changes in the temperature field.

Fig. 6 shows the transient response of the average Nusselt number with $H = 1$, $D = 0.9$ and $Ra = 100$ where oscillatory convection is found at some values of Pe. The sudden heating of the lower element is imposed and the average Nusselt number is calculated, which show very high value at the first time step. This is evident in any suddenly heated convection problem. With increasing the time the average Nusselt number goes down and then increased to reaches its steady state value for low Pe as shown in Fig. 6 ($Pe = 1$ and $Pe = 3$). Fig. 6 shows the steady state can be achieved for $Pe = 10$ also after small oscillations. While, for $Pe = 5$ and $Pe = 7$ the oscillation of $\overline{Nu}$ is a periodic oscillation and no steady state value of $\overline{Nu}$ can be found. Fig. 6 shows the steady state value of $\overline{Nu}$ when $Pe = 1$ is higher than that when $Pe = 3$ and $Pe = 10$. This indicates mixed convection mode as that presented in Fig. 2. Therefore, the oscillatory convection is expected in the mixed convection mode at some values of Pe, which are depending on the other parameters H, D and Ra. Table 2 shows the conditions at which the oscillatory convection occurring with fixed $H = 1$. It can be observed form Table 2 that oscillatory convection occurring at high values of Ra and D and the range of Pe at which the oscillatory convection occurring is reducing with the reduction of Ra.

The isotherms and the streamlines are shown in Fig. 7 for the oscillatory convection case discussed above with $Pe = 5$. The isotherms and the streamlines are shown for three time steps, when $\overline{Nu}$ is maximum, minimum and approximately average. At time steps when $\overline{Nu}$ shows maximum, Fig. 7(a) shows the jet flow is reaching the heated element and the isotherms show the gradients near the element, which leads to the increase in $\overline{Nu}$. The streamlines show that there is another anticlockwise rotating cell near the heated element due to buoyancy. At the time step when the $\overline{Nu}$ have approximately average value (Fig. 7(b)) the anticlockwise rotating cell near the heated element due to buoyancy is enlarged and moved to rotate the fluid above the heated element. The gradients of the isotherms near the heated element are changed to be approximately parallel to heat source. While at the time when $\overline{Nu}$ shows minimum value (Fig. 7(c)), the streamlines show the anticlockwise rotating cell near the heated element starting to move away from the heat source and forming a stagnation region above around half of its length. The isotherms in this case show parallel lines to the horizontal indicating

Table 2
Ranges of Pe at which the oscillatory convection occurring with $H = 1$

$Ra\backslash D$	0.9	0.8	0.7	0.6	0.5	0.4	0.3
100	$4 \rightarrow 9$	$4 \rightarrow 9$	$5 \rightarrow 12$	$6 \rightarrow 13$	$7 \rightarrow 15$	$9 \rightarrow 17$	$16 \rightarrow 20$
90	$4 \rightarrow 8$	$4 \rightarrow 9$	$5 \rightarrow 11$	$6 \rightarrow 12$	$7 \rightarrow 13$	$9 \rightarrow 15$	–
80	$4 \rightarrow 8$	$4 \rightarrow 9$	$5 \rightarrow 9$	$6 \rightarrow 10$	$7 \rightarrow 10$	9	–
70	$4 \rightarrow 6$	$4 \rightarrow 7$	$5 \rightarrow 7$	$6 \rightarrow 7$	–	–	–

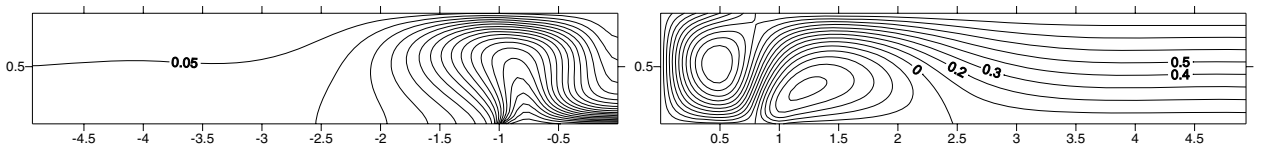

(a) At time steps when $\overline{Nu}$ = 3.648 (maximum)

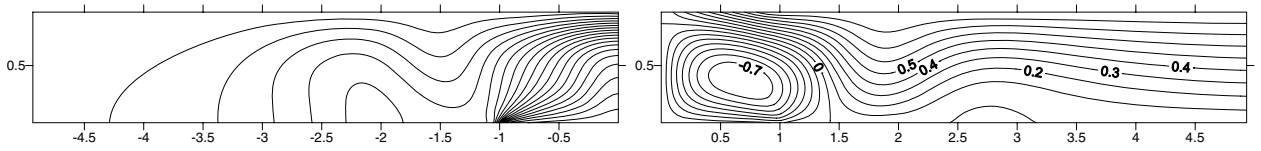

(b) At time steps when $\overline{Nu}$ = 2.829 (approximately average)

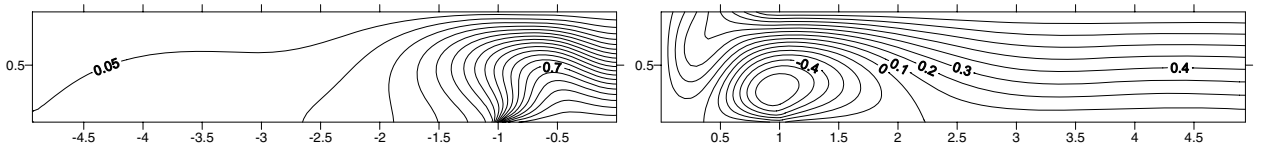

(c) At time steps when $\overline{Nu}$ = 2.138 (minimum)

Fig. 7. Isotherms (left), streamlines (right) for oscillatory condition with $H = 1.0$, $D = 0.9$, $Ra = 100$ and $Pe = 5$ ($\Delta\Psi = 0.1$, $\Delta\theta = 0.05$).

the conduction mode of heat transfer. It can be seen from Fig. 7 the oscillation of the direction of the jet, from turning left and right during the oscillatory convection.

6. Conclusions

The jet impingement cooling of heated portion of a horizontal surface immersed in a fluid saturated porous media is investigated numerically. The external jet flow and the buoyancy driven flow are chosen to be in opposite direction. The dimensionless governing parameters results from the mathematical model are the Rayleigh number, Péclet number, jet width and the distance between the jet and the heated portion normalized to the length of the heated element. After validation of the numerical method, the results are presented in the mixed convection regime with wide ranges of the governing parameters with the limitation of the Darcy model. The numerical results are presented as average Nusselt number along the heated element against Péclet number for different values of the governing parameters. It is found for high values of Péclet number that increasing either the Rayleigh number or jet width increases the average Nusselt number. Narrowing the distance between the jet and the heated portion could increase the average Nusselt number. The values of average Nusselt number show minimum values for some values of Péclet number for mixed convection conditions. The value of Pe at which minimum $\overline{Nu}$ occurs depends on Ra and at low values of Ra this case where $\overline{Nu}$ shows minimum value is not obvious. No steady-state solution can be found in some cases; when the external jet flow and the flow due to buoyancy are in conflict for domination. The results from the unsteady governing equations in these cases show oscillation of the average Nusselt number along the heated element with the time without reaching steady state.

References

[1] D.A. Nield, A. Bejan, Convection in Porous Media, second ed., Springer, New York, 1999.
[2] K. Vafai (Ed.), Handbook of Porous Media, Marcel Dekker, New York, 2000.
[3] M. Kaviany, Principles of Heat Transfer in Porous Media, second ed., Springer, New York, 1995.
[4] I. Pop, D.B. Ingham, Convective Heat Transfer: Mathematical and Computational Modelling of Viscous Fluids and Porous Media, Pergamon, Oxford, 2001.
[5] B. Gebhart, Y. Jaluria, R.L. Mahajan, B. Sammakia, Buoyancy-Induced Flows and Transport, Hemisphere, New York, 1988.

[6] P. Cheng, I-Dee Chang, Buoyancy induced flows in a saturated porous medium adjacent to impermeable horizontal surfaces, Int. J. Heat Mass Transfer 19 (1976) 1267–1272.
[7] C.H. Johnson, P. Cheng, Possible similarity solution for free convection boundary layers adjacent to flat plates in porous media, Int. J. Heat Mass Transfer 21 (1978) 709–718.
[8] C.T. Hsu, P. Cheng, Vortex instability of mixed convection flow in a semi-infinite porous medium bounded by a horizontal surface, Int. J. Heat Mass Transfer 23 (1980) 789–798.
[9] W.J. Minkowycz, P. Cheng, R.N. Hirschberg, Non-similarity boundary layer analysis of mixed convection about a horizontal heated surface in a fluid-saturated porous medium, Int. Commun. Heat Mass Transfer 11 (1984) 127–141.
[10] F.C. Lai, F.A. Kulacki, The influence of surface mass flux on mixed convection over horizontal plates in saturated porous media, Int. J. Heat Mass Transfer 33 (1990) 576–579.
[11] T.K. Aldoss, T.S. Chen, B.F. Armaly, Nonsimilarity solutions for mixed convection from horizontal surfaces in porous medium-variable wall temperature, Int. J. Heat Mass Transfer 36 (1993) 471–477.
[12] V. Prasad, F.A. Kulacki, Natural convection in horizontal porous layers with localized heating from below, ASME J. Heat Transfer 109 (1987) 795–798.
[13] V. Prasad, F.C. Lai, F.A. Kulacki, Mixed convection in horizontal porous layer heat from below, ASME J. Heat Transfer 110 (1988) 395–402.
[14] F.C. Lai, C.Y. Choi, F.A. Kulacki, Free and mixed convection in horizontal porous layers with multiple heat sources, J. Thermophys. 4 (1990) 221–227.
[15] I. Sezai, A.A. Mohamad, 3-D simulation of laminar rectangular impinging jets, flow structure and heat transfer, ASME J. Heat Transfer 121 (1999) 50–56.
[16] L.B.Y. Aldabbagh, I. Sezai, A.A. Mohamad, Three-dimensional investigation of a laminar impinging square jet interaction with cross-flow, ASME J. Heat Transfer 125 (2003) 243–249.
[17] X. Li, J.L. Gaddis, T. Wang, Multiple flow patterns and heat transfer in confined jet impingement, Int. J. Heat Fluid Flow 26 (2005) 746–754.
[18] M. Prakash, O.F. Turan, Y. Li, J. Mahoney, G.R. Thorpe, Impinging round jet studies in a cylindrical enclosure with and without a porous layer: Part I—Flow visualizations and simulations, Chem. Eng. Sci. 56 (2001) 3855–3878.
[19] W.S. Fu, H.C. Huang, Thermal performance of different shape porous blocks under an impinging jet, Int. J. Heat Mass Transfer 40 (1997) 2261–2272.
[20] T.M. Jeng, S.C. Tzeng, Numerical study of confined slot jet impinging on porous metallic foam heat sink, Int. J. Heat Mass Transfer 48 (2005) 4685–4694.
[21] S.V. Patankar, Numerical Heat Transfer and Fluid Flow, McGraw-Hill, New York, 1980.
[22] T. Hayase, J.A.C. Humphrey, R. Greif, A consistently formulated QUICK scheme for fast and stable convergence using finite-volume iterative calculation procedures, J. Comput. Phys. 98 (1992) 108–118.
[23] N.H. Saeid, Analysis of mixed convection in a vertical porous layer using non equilibrium model, Int. J. Heat Mass Transfer 47 (2004) 5619–5627.
[24] N.H. Saeid, A.A. Mohamad, Natural convection in a porous cavity with spatial sidewall temperature variation, Int. J. Numer. Methods Heat Fluid Flow 15 (2005) 555–566.
[25] N.H. Saeid, Natural convection from two thermal sources in vertical porous layer, ASME J. Heat Transfer 128 (2006) 104–109.
[26] F.C. Lai, F.A. Kulacki, Oscillatory mixed convection in horizontal porous layers heated from below, Int. J. Heat Mass Transfer 34 (1991) 887–890.